

## NEW CFD BASED MODEL FOR THE DESIGN AND OPTIMISATION OF ELECTROSTATIC PRECIPITATORS FOR BIOMASS COMBUSTION PLANTS

M. Blank<sup>1</sup>, M. Schöffl<sup>2</sup>, R. Scharler<sup>1,2</sup>, I. Obernberger<sup>1,2</sup>

<sup>1</sup>BIOS BIOENERGIESYSTEME GmbH

Inffeldgasse 21b, 8010 Graz, Austria

Tel.: +43 (0)316 481300 15, Fax: +43 (0)316 481300 4; E-mail: blank@bios-bioenergy.at

<sup>2</sup>Institute for Process and Particle Engineering

Graz University of Technology, Inffeldgasse 13, 8010 Graz, Austria

**ABSTRACT:** A Computational Fluid Dynamics (CFD) model has been developed that allows a realistic calculation of the precipitation efficiency of tube electrostatic precipitators, which are designed for use in residential biomass heating plants. The motivation for this work is especially the steady decrease of particle emission limits, which increases the interest in the application of cost-effective electrostatic precipitators for small biomass boilers. The details of the model are described. For validation, the model has been applied to a small-scale electrostatic precipitator, and the results of the simulation are compared to the data of corresponding test runs. Good agreement is found between simulation and measurements.

**Keywords:** computational fluid dynamics (CFD), modelling, electrostatic precipitator, gas cleaning, biomass, combustion.

### 1 INTRODUCTION

Electrostatic precipitators are among the most important devices for the separation of particles from the fluid flow. They are mainly applied for cleaning large gas streams, for example in large power plants, the steel industry, waste-to-energy plants, or chemical industry. However, due to the efforts to reduce particle emissions, the respective limits are steadily decreasing, and cost- and energy efficient filtering technologies become increasingly interesting also in small-scale applications, such as residential biomass heating plants.

In order to achieve a maximum efficiency of an electrostatic precipitator, the geometry, the electrode and other operational parameters of the device have to be optimised. For this reason, a Computational Fluid Dynamics (CFD) model has been developed [1] that allows a realistic calculation of the precipitation efficiency of tube electrostatic precipitators, which are designed for residential biomass heating plants. This new CFD model allows the evaluation of existing electrostatic precipitators as well as an optimisation of their geometry, primarily of the discharge- and the collecting electrode. In addition, newly developed electrostatic precipitators can be evaluated by CFD simulations and the collection efficiency can be verified before the testing phase starts, thereby reducing the costs of development.

In order to validate the model, a small-scale tube electrostatic precipitator designed for use with a biomass boiler was considered. For the same system, test runs were performed, such that the simulated precipitation efficiencies can be directly compared to measured data.

This paper is organised as follows: In Sec. 2, the new CFD model for the electrostatic precipitator is described in detail, with some background given in Sec. 2.1 and the details of the model in Secs. 2.2-2.4. The test case used for validation is presented in Sec. 3. Simulation results, discussion, and comparison to the measured data are reported in Sec. 4. Conclusions and outlook are given in Sec. 5.

### 2 DESCRIPTION OF THE MODEL

#### 2.1 Background

In an electrostatic precipitator, an electric field builds up between the discharge electrode, where a high voltage is applied, and the collecting electrode. This field is responsible for the particle separation, because dust particles are charged while moving through the electric field, and then deflected towards the collecting electrode.

In the case of biomass combustion, several different kinds of particles with different properties, such as density, relative permittivity, dust resistance and particle size distributions have to be considered. The most important species are salt, tar and soot particles, which make up the fine dust (aerosol) fraction, and coarse fly ash (mineral particles mostly composed of Ca, Mg, Si, K, Al and Fe in oxidised form).

Another effect which has to be taken into account in the model described here is the formation of a spatially distributed ion charge density: due to the influence of the electric field, the gas in the precipitator gets partly ionised, and the resulting charge density causes a coupling between the flue gas flow and the electric field.

Thus, the system contains three main components: the gas flow, the dust particles, and the electric field, whose mutual influences have to be included in the CFD model. The implementation was done in the framework of the commercial CFD software ANSYS Fluent, which was extended for this purpose via so-called "user defined functions" (UDFs).

#### 2.2 Modelling of the flue gas flow

For describing the flue gas flow in the electrostatic precipitator, the model relies mainly on the built-in features of ANSYS Fluent. The basic fluid flow is determined by the momentum equation for the fluid, which in the presence of an electric field  $\vec{E}$  reads (cf. [2])

$$\vec{u} \cdot \nabla \vec{u} + \frac{\nabla p}{\rho_f} - \mu \nabla^2 \vec{u} = \rho_{ion}^{el} \vec{E}.$$

The terms on the left-hand-side of the equation describe the convection of the fluid (with fluid velocity  $\vec{u}$ ), the contribution of the pressure  $p$  ( $\rho_f$  stands for the

fluid density) and of viscous transport (with fluid viscosity  $\mu$ ). These terms are an integral part of ANSYS Fluent, whereas the term on the right-hand-side, that describes the electric force acting on the partly ionised gas (ion charge density  $\rho_{ion}^{el}$ ), is included as a custom source term. In order to obtain a consistent solution, the mass continuity equation,

$$\nabla \cdot \vec{u} = 0,$$

has to be satisfied in addition to the momentum equation inside the whole fluid domain.

To describe the situation in an electrostatic precipitator, other models have to be coupled to those basic equations. Especially, since the flow is (moderately) turbulent, the SST (shear stress transport)  $k-\omega$  turbulence model was used, which is a built-in part of ANSYS Fluent. The flue gas itself is modelled as a mixture of  $O_2$ ,  $CO_2$ ,  $H_2O$ , and  $N_2$ , which are the most important chemical species after complete burn-out of the fuel.

### 2.3 Modelling of the electric field

According to the equations of electrodynamics, the electric field is given as the gradient of the electrostatic potential  $\Phi$

$$\vec{E} = -\nabla\Phi,$$

which in turn is described via the Poisson equation

$$\nabla^2\Phi = -\frac{\rho_{ion}^{el} + \rho_{part}^{el}}{\epsilon_0}.$$

The electric charge densities (the ion charge density  $\rho_{ion}^{el}$  and charge density of the dust particles  $\rho_{part}^{el}$ ) act as sources for the field. While the charges of the dust particles are calculated using a model ("field modified diffusion model", see section 2.4), the spatial ion charge density is determined via a continuity equation describing the conservation of electric charge,

$$\nabla \cdot (\rho_{ion}^{el} b_{ion} \vec{E}) = 0,$$

where  $b_{ion}$  is the ion mobility in the flue gas.

In addition, an estimate of the ion charge density on the discharge electrode is necessary as a boundary condition. In order to calculate its value, the local ion charge density inside the electrostatic precipitator on a cylinder enclosing the discharge electrode may be approximated by [3]

$$\rho_{ion}^{el} = \frac{I}{2\pi r_z l b_{ion} E},$$

where diffusive as well as convective ion transport have been neglected. The magnitude of the ion charge density depends on the radius of the enclosing cylinder  $r_z$ , its length  $l$ , and the ion mobility  $b_{ion}$  as well as the magnitude of the local electric field strength denoted by  $E$ . In addition, the electric current  $I$  is needed, which can be taken from the current-voltage characteristic of the precipitator at the operating voltage. During the setup of the simulation, the boundary condition for  $\rho_{ion}^{el}$  is adjusted iteratively, such that the simulated ion charge density on the cylinder around the discharge electrode agrees with the value obtained from the above equation.

In this way, all electric quantities (potential, electric field, spatial ion charge density) can be fully described and modelled in the CFD framework.

### 2.4 Modelling of the dust particles

In biomass combustion plants, several types of dust particles are of relevance: the fine dust (PM1 fraction, aerosols), which consists of salt, soot and tar particles as well as the coarse fly ash fraction (see Fig. 1 for a typical particle size distribution). For all of these different particles, the specific particle properties, such as particles density, particle size distributions, as well as electrical properties (relative permittivity) are considered in the CFD model. The relevant parameters are displayed in Tab. I.

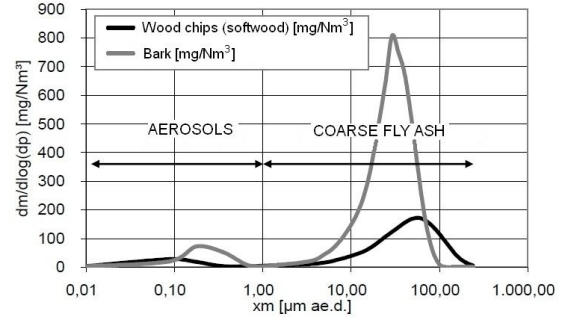


**Figure 1:** Typical particle size distribution of total dust for large-scale biomass combustion plants [4]; Note that for small-scale combustion plants, the aerosols are the dominant fraction.

**Table I:** Properties of the particle species considered in the simulation

Salts		
density [kg/m <sup>3</sup> ]	2300	[5],[6]
relative permittivity [-]	5	[7],[8]
Tar		
density [kg/m <sup>3</sup> ]	1100	[9]
relative permittivity [-]	4	[7]
Soot		
density [kg/m <sup>3</sup> ]	1700	[10]
relative permittivity [-]	19	[7]
Coarse fly ash		
density [kg/m <sup>3</sup> ]	2500	[11]
relative permittivity [-]	5	[7],[8]

The dust particles are modelled via the discrete phase model (DPM), which is part of ANSYS Fluent. This model consistently describes the motion of the particles through the fluid flow by solving the equation of motion for the particles,

$$\frac{d\vec{u}_p}{dt} = F_D(\vec{u} - \vec{u}_p) + (1 - \frac{\rho_f}{\rho_p})\vec{g} + \vec{F}_{el}.$$

The change of the particle velocity  $\vec{u}_p$  with time is given by the drag force  $F_D(\vec{u} - \vec{u}_p)$  plus the gravitational force  $(1 - \frac{\rho_f}{\rho_p})\vec{g}$ , both of which can easily be activated in ANSYS Fluent.

The additional electric force,

$$\vec{F}_{el} = \frac{1}{m} q_p \vec{E}$$

(with particle mass  $m$ , particle charge  $q_p$ , and

particle mass density  $\rho_p$ ), is added using the UDF framework.

This force mediates the coupling between the electric field and the particles via their charge. The particle charge is calculated with a charging model, the ‘‘Field modified diffusion model’’, and given by

$$q_p = \begin{cases} \frac{q_{p,\infty}}{\tau_Q} \left(1 - \frac{q_p}{q_{p,\infty}}\right)^2 t + a(\tilde{E}) \frac{8\pi \varepsilon_0 k T d_p}{e^- \tau_Q} t & \text{for } q_p \leq q_{p,\infty} \\ \frac{4a(\tilde{E})}{\tau_Q} \frac{q_p - q_{p,\infty}}{\exp\left(\frac{(q_p - q_{p,\infty})e^-}{2\pi \varepsilon_0 k T d_p}\right) - 1} t & \text{for } q_p > q_{p,\infty} \end{cases}$$

This approach combines two charging mechanisms, namely the charging via the interaction with the electric field (corresponding to the first term in the first line of the equation) and the charging by diffusion (see, e.g., [2] for details on the model).

### 3 TEST CASE USED FOR VALIDATION

For the validation of the newly developed model a tube electrostatic precipitator (shown in Fig. 2) was considered. It operates with a high voltage of 15 kV and has a discharge electrode with a saw-tooth profile. The filter is designed for pellet boilers with a nominal power of up to 26 kW and is equipped with an automatic cleaning system.

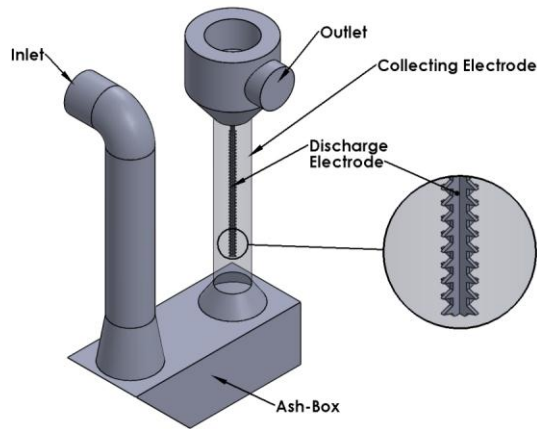


**Figure 2:** 3D geometry of the tube electrostatic precipitator used for the validation of the CFD model

Several test runs were performed with this filter mounted on a pellet boiler with a nominal power of 15 kW. At nominal load, the volumetric flow rate through the filter was 40 m<sup>3</sup>/h with a flue gas temperature of 101 °C at the filter inlet (for the flue gas composition, see Tab. II). Simultaneously, data on the dust load and precipitation efficiency were collected by parallel measurements upstream and downstream of the filter. The measurement of the total dust load was performed according to VDI 2066, the aerosol fraction was analysed with low-pressure Berner-type impactors as well as with an electric impactor. The resulting total dust load amounted to 12.9 mg/Nm<sup>3</sup> at 13 Vol% O<sub>2</sub> (dry flue gas), while the fine dust load (PM1 fraction) was 6.2 mg/Nm<sup>3</sup> at 13 Vol% O<sub>2</sub> (dry flue gas).

**Table II:** Flue gas composition (the concentration of CO in the flue gas is below 50 mg/Nm<sup>3</sup>, dry flue gas, 13Vol% O<sub>2</sub>, and has therefore been neglected.)

Species	Mole fraction [% wet flue gas]
O <sub>2</sub>	7.3
H <sub>2</sub> O	10.0
CO <sub>2</sub>	11.2
N <sub>2</sub>	71.5

The impactor charges have been subsequently analysed to extract the amount of soot, salts and tars in the particulate emissions. The resulting distributions are shown in Fig. 3 and Fig. 4. Due to the almost complete burnout of the flue gas (CO below 50 mg/Nm<sup>3</sup>, dry flue gas, 13 Vol% O<sub>2</sub>), the amount of tars and soot in the particles is low.

These parameters were used as input for the CFD simulation. The simulation itself contains no time dependence, and thus corresponds to a stationary phase of operation of the filter.

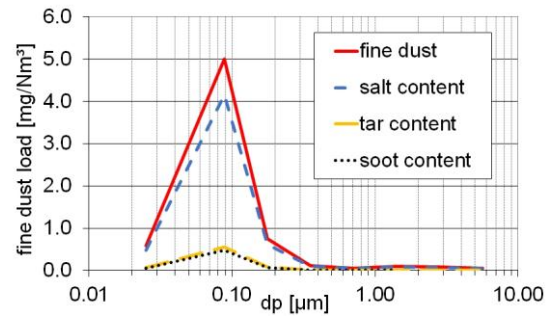


**Figure 3:** Measured particle size distribution of the fine dust and its components used for the simulation

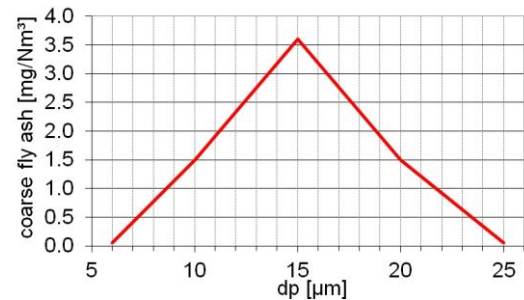


**Figure 4:** Measured particle size distribution of the coarse fly ash used for the simulation

## 4 SIMULATION RESULTS AND DISCUSSION

### 4.1 Flow of the flue gas and electric quantities

The simulated velocities in the electrostatic precipitator (shown in Fig. 5) do not deviate from the expected behaviour. At the entrance to the actual filter, the velocities are around 1.5 m/s (reduction of diameter compared to the ash box). The highest flow velocities (maximum: 2.12 m/s) occur near the discharge electrode, showing the combined effects of the electric field and the accelerating dust particles on the flow velocity. Before reaching the outlet of the filter, the velocities decrease again due to the larger diameter.

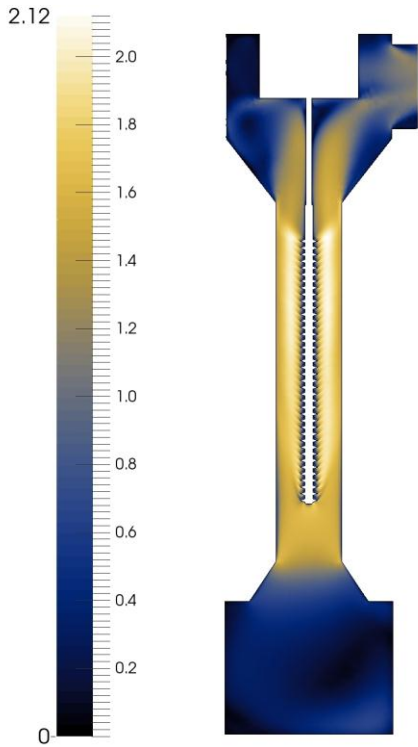


**Figure 5:** Contours of the flue gas velocity [m/s] in a vertical section through the precipitator

The electric quantities calculated in the electrostatic precipitator are shown in Fig. 6. The electrostatic potential decreases from the discharge to the collecting electrode. In accordance with the boundary conditions, its value varies from 15 kV at the discharge electrode to 0 kV at the collecting electrode. As described in Sec. 2.3, the electric field is calculated as the gradient of the potential. As expected, its magnitude is highest in the vicinity of the discharge electrode, where the effect of the saw-tooth geometry on the field is clearly resolved. The electric field also shows irregularities (visible as streaks), which are caused by the effects of the charged dust particles on the field. The distribution of the ion charge density also does not deviate from the expected behaviour: its biggest values are located around the discharge electrode, and it is decreasing in outwards direction.

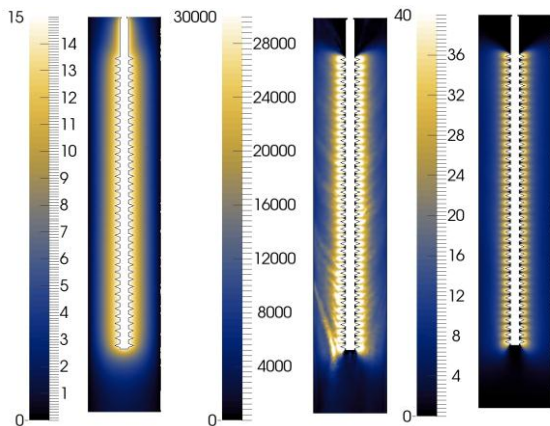


**Figure 6:** Contours of the electrostatic potential [kV] (left), the electric field [kV/m] (centre), and the spatial ion charge density [ $10^{-5} C/m^3$ ] (right) in a vertical section

through the precipitator

#### 4.2 Movement of the dust particles

The dust particles are transported through the filter along with the flue gas flow. As soon as they enter the domain of the collecting- and discharge electrode (i.e., the filter), the particles start to build up electric charge according to the model described in Sec. 2.4. Along their path, they are deflected by the electric field towards the collecting electrode, and consequently accelerated outwards, where they are trapped on the collecting electrode. Fig. 7 shows a selection of particle tracks in the precipitator, which illustrate this behaviour. Especially in the “Top view” (Fig. 7, right) the outwards movement and acceleration is clearly visible.

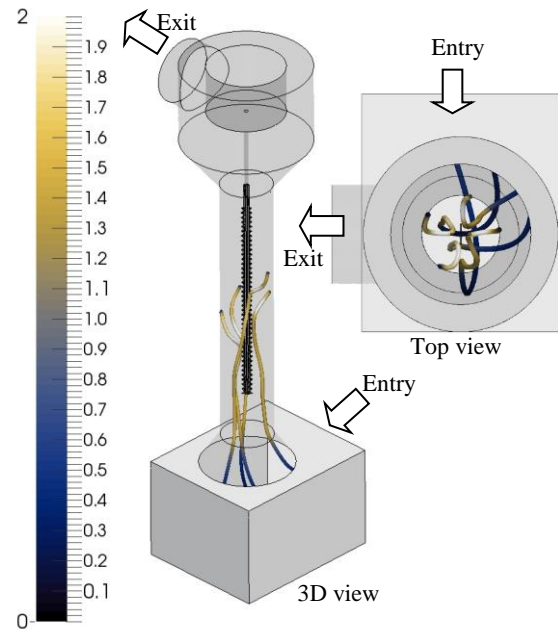


**Figure 7:** Particle tracks in the electrostatic precipitator (selection), coloured by the particle velocity [m/s]

#### 4.3 Precipitation efficiency

The results obtained with the CFD model are in good agreement with the corresponding measured values. For the PM1 fraction of the dust particles, which typically represents the biggest fraction of the total dust (about 90%) for residential biomass heating plants, the simulated collection efficiency of 79.6% is in very good agreement with the measured value of (82 +/- 5)%. For the total dust, the simulated collection efficiency amounts to 87.8% (measurement: (88.4 +/- 3)%), see Fig. 8).

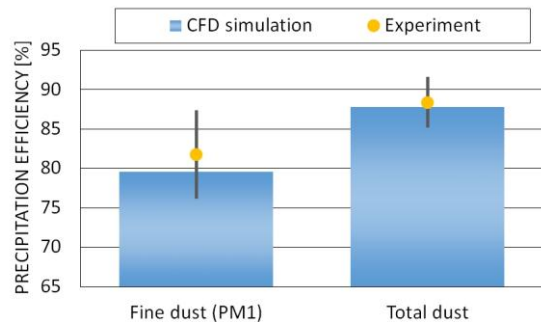


**Figure 8:** Simulated precipitation efficiencies of fine dust and total dust compared to experimental data

**Table III:** Precipitation efficiencies for each species considered in the simulation

Precipitation efficiency	CFD simulation	Measurement
Salts	79.9 %	n.a.
Soot	15.9 %	n.a.
Tar	77.5 %	n.a.
Coarse fly ash	99.7 %	n.a.
Fine dust (PM1)	79.6 %	(81.8 +/- 5) %
Total dust	87.8 %	(88.4 +/- 3) %

In contrast to the PM1 fraction, the simulated collection efficiency for the total dust is generally higher. This is due to the larger particle size of coarse fly ash particles, which are almost fully collected in the electrostatic precipitator (99.7% precipitation efficiency, cf. Tab. III).

Concerning the collection efficiency of the individual kinds of particles (salts, tars and soot, see also Tab. III), the results obtained are in good agreement with a comparable test run taken from literature [12]. The collection efficiencies of salt and tar particles can be simulated well and are in general higher than for soot, which shows re-entrainment. This is caused by agglomeration of soot particles on the collecting electrode, which may lose their electric charges due to the high relative permittivity. Therefore, a large fraction of the already collected particles can leave the collecting electrode and be re-entrained into the flue gas. As a further complication, the agglomeration process significantly alters the particle size distribution. These effects cannot be modelled directly at this stage, therefore a re-entrainment rate of 80% (i.e. 80% of the collected soot particles are re-entrained into the flue gas) has been considered based on measurement data.

The simulation results for the fractional collection efficiency (cf. Fig. 9) show a minimum around a particle diameter of 0.5  $\mu\text{m}$ . In general, the resulting curve behaves as expected (see e.g. [12]), and thus serves as a further indication that the new CFD model correctly predicts the separation of particles in an electrostatic precipitator.

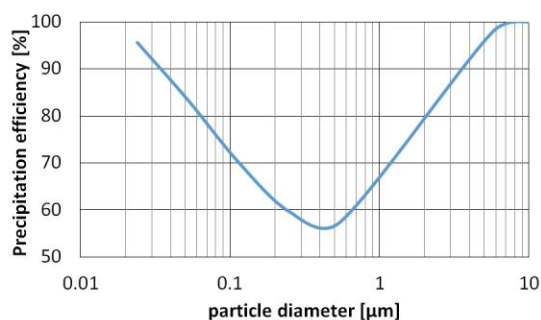


**Figure 9:** Precipitation efficiency for the total dust vs. the particle diameter [ $\mu\text{m}$ ]

## 5 CONCLUSIONS AND OUTLOOK

In this work, a 3D CFD model for the simulation of the flow and particle separation in an electric field has been developed. The flow velocities and the electric quantities (electrostatic potential, electric field, and ion charge density) behave as expected. Most importantly, the simulated precipitation efficiencies show good agreement with measurements, and the fractional

collection efficiency as well as the collection efficiencies for the separate species considered follow the expected patterns.

The largest uncertainty in this model is the re-entrainment of soot particles into the flue gas, where empirical adjustments were necessary.

The novel CFD model presented here opens up the opportunity for evaluation and optimisation of electrostatic precipitator geometries. In addition, sensitivity analyses can be performed: The high voltage can be varied, or the influences of the flow velocity and the flue gas temperature/water content on the precipitation efficiency can be studied. Another possibility is the analysis of the effects of depositions on the collecting electrode on the precipitation behaviour.

In the future, the newly developed CFD-model can therefore be used as a valuable tool for the development and optimisation of electrostatic precipitator geometries.

## 6 REFERENCES

- [1] Schöffl, M. 2014: Entwicklung eines CFD-Modells für die Simulation von Elektrofiltern für Biomasse-Feuerungsanlagen, Diploma thesis, Graz University of Technology.
- [2] Horn, M. 2010: Zur Modellierung partikulärer elektro-fluiddynamischer Strömungen, Ph.D. thesis, University Erlangen.
- [3] Lübbert, C. 2011: Zur Charakterisierung des gequenchten Zustandes im Elektroabscheider, Ph.D. thesis, University Cottbus.
- [4] Obernberger, I. et al. 2007: Feinstaubemissionen aus Pelletfeuerungen – aktueller Stand der Erkenntnisse. In: Tagungsband zu den World Sustainable Energy days, O.Ö. Energiesparverband (Ed.), Wels.
- [5] Jöller, M. 2008: Modelling of aerosol formation and behaviour in fixed-bed biomass combustion systems, Dissertation, Universität Graz.
- [6] Brunner, T. 2006: Aerosols and coarse fly ashes in fixed-bed biomass combustion. In: Series Thermal Biomass Utilization, Band 7, ISBN 3-9501980-4-0, Graz.
- [7] Holdefer, M. 1999: Relative Dielektrizitätskonstante  $\epsilon_r$  von flüssigen und festen Medien (DK-Werte), Weil am Rhein.
- [8] Oguchi, T. et al. 2009: Measurements of dielectric constant of volcanic ash erupted from five volcanoes in Japan. In: Transactions on geoscience and remote sensing, ISSN 0196-2892, S. 1089-1096, Yokohama.
- [9] Morf, P.; Nussbaumer T. 1998: Grundlagen zur Teerbildung bei der Holzvergasung, Zürich.
- [10] Chemical Book Inc.: Chemical Book, 2008, [http://www.chemicalbook.com/ProductChemicalPropertiesCB2767903\\_EN.htm](http://www.chemicalbook.com/ProductChemicalPropertiesCB2767903_EN.htm), access date 2015/05/19.
- [11] Wang, S. et al. 2006: Biomass fly ash in concrete - Mixture, proportioning and mechanical properties. In: Fuel, Vol 87, Provo.
- [12] Nussbaumer, T. 2010: Potential und Technik zur Holzenergie-Nutzung, ISBN 3-908705-21-5, Zürich.

